Received: 12 November 2020 | Revised: 21 February 2021 | Accepted: 22 February 2021

DOI: 10.1111/epi.16868

Epilepsia®

FULL-LENGTH ORIGINAL RESEARCH

Defining the latent period of epileptogenesis and epileptogenic zone in a focal cortical dysplasia type II (FCDII) rat model

Hsin-Yi Kao[1] | **Shuntong Hu**[1,2] | **Temenuzhka Mihaylova**[1] | **Julie Ziobro**[3] | **EunSeon Ahn**[4] | **Carli Fine**[4] | **David Brang**[4] | **Brendon O. Watson**[5,6] | **Yu Wang**[1]

[1]Department of Neurology, University of Michigan, Ann Arbor, USA

[2]Department of Neurology, the Third Xiangya Hospital, Central South University, Changsha, China

[3]Department of Pediatrics, University of Michigan, Ann Arbor, USA

[4]Department of Psychology, University of Michigan, Ann Arbor, USA

[5]Department of Psychiatry, University of Michigan, Ann Arbor, USA

[6]Molecular and Behavioral Neuroscience Institute, University of Michigan, Ann Arbor, USA

Correspondence
Yu Wang, Department of Neurology, 5025 BSRB, 109 Zina Pitcher Place, Ann Arbor, MI, 48109-2200.
Email: eegwang@med.umich.edu

Funding information
National Institute of Neurological Disorders and Stroke, Grant/Award Number: K08NS099379, R01NS113824 and U54NS117170

Summary

Objectives: Focal cortical dysplasia type II (FCDII) is one of the most common underlying pathologies in patients with drug-resistant epilepsy. However, mechanistic understanding of FCDII fails to keep pace with genetic discoveries, primarily due to the significant challenge in developing a clinically relevant animal model. Conceptually and clinically important questions, such as the unknown latent period of epileptogenesis and the controversial epileptogenic zone, remain unknown in all experimental FCDII animal models, making it even more challenging to investigate the underlying epileptogenic mechanisms.

Methods: In this study, we used continuous video-electroencephalography (EEG) monitoring to detect the earliest interictal and ictal events in a clustered regularly interspaced short palindromic repeats (CRISPR)-in utero electroporation (IUE) FCDII rat model that shares genetic, pathological, and electroclinical signatures with those observed in humans. We then took advantage of in vivo local field potential (LFP) recordings to localize the epileptogenic zone in these animals.

Results: To the best of our knowledge, we showed for the first time that epileptiform discharges emerged during the third postnatal week, and that the first seizure occurred as early as during the fourth postnatal week. We also showed that both interictal and ictal discharges are localized within the dysplastic cortex, concordant with human clinical data.

Significance: Together, our work identified the temporal and spatial frame of epileptogenesis in a highly clinically relevant FCDII animal model, paving the way for mechanistic studies at molecular, cellular, and circuitry levels.

KEYWORDS
epileptogenic zone, FCDII, latent period

Key points

- We generated a highly clinically relevant focal cortical dysplasia type II (FCDII) rat model to investigate the latent period of epileptogenesis and epileptogenic zone.
- We showed for the first time that epileptiform discharges emerged during the third postnatal week, and that the first seizure occurred during the fourth postnatal week.

- We showed that both interictal and ictal discharges were localized within the dysplastic cortex, concordant with human clinical data.

1 | INTRODUCTION

Extensive clinical and basic science studies on mesial temporal lobe epilepsy (mTLE)/hippocampal sclerosis (HS) have generated exceptional knowledge in epilepsy at the genetic, molecular, and circuitry levels.[1] However, focal neocortical epilepsies have different anatomo-electroclinical manifestations and epileptogenic pathophysiology.[2] Their epileptogenesis and intractability remain poorly understood primarily due to the challenges in developing focal cortical dysplasia (FCD) animal models that recapitulate the genetics, pathology, and electroclinical expression. For example, acute seizure models using chemo-convulsants and chronic epilepsy models induced by freeze-lesion or tetanus toxin (TTX)[3] have limited translatability because human neocortex epilepsies have a different pathogenesis. On the other hand, transgenic animals lack a focal lesion and often do not have spontaneous seizures.[4]

Focal cortical dysplasia (or FCD) is a common cause of refractory focal epilepsies (FEs). As the most common underlying pathology in children with refractory FEs, it accounted for 26.8% of those cases in a series of ~2600 specimens of brain tissue obtained during epilepsy surgery.[5,6] FCD type II (FCDII) is firmly linked to low-frequency somatic mutations within mammalian target of rapamycin (mTOR) signaling pathways.[7] *DEPDC5* mutations have been identified as the most common cause in familial focal epilepsies.[8,9] In addition, its second-hit somatic mutations have been discovered in FCDII tissues resected from patients with refractory focal epilepsies.[10,11] The product of *DEPDC5*, pleckstrin (DEP) domain-containing protein 5 (DEPDC5), a key regulator of the amino acid–sensing machinery in the mTOR signaling pathway, inhibits mTORC1 recruitment to lysosomal membranes and therefore inhibits mTORC1-mediated phosphorylation of S6 kinase and its substrate S6.[12] Recently we have generated a novel FCDII rat model using *Depdc5* Clustered Regularly Interspaced Short Palindromic Repeats-in utero electroporation clustered regularly interspaced short palindromic repeats (CRISPR)-in utero electroporation (IUE) to introduce *indels* in rat dorsal telencephalic progenitors. These animals have a focal dysplastic cortex, and 100% of these animals display frequent focal interictal and ictal discharges that are highly similar to those recorded in human FCDII, such as electrographic hallmarks of human FCD including frequent paroxysmal fast activity (PFA), rhythmic spikes (RS), and periodic epileptiform discharges (PEDs).[5] Because seizure itself generates widespread and sustained cellular and molecular changes, the timeframe of the latent period (delay to the first seizures) needs to be defined first to investigate epileptogenic mechanisms underlying the dysplastic cortex. In addition, because seizure-propagating sites have different electrographic and cellular signatures,[13] the seizure-onset site also needs to be defined to construct a logic circuitry and molecular network underpinning the hyperexcitable cortex. Unfortunately, these two conceptually critical questions remain unknown in all FCD-related epilepsy models, making it difficult to understand its epileptogenicity and develop mechanistic-based therapies.

2 | METHODS

2.1 | Plasmids, IUE, and animals

Depdc5 CRISPR-IUE animals were generated as described previously (Figure 1A).[5] All animal studies were approved by the University of Michigan Institutional Animal Care and Use Committee.

2.2 | Long-term EEG recording and analysis

To determine the latent period of epileptogenesis in *Depdc5* CRISPR-IUE rats, we) monitored animals with long-term video-EEG (electroencephalography) recording. Because our pilot studies did not detect epileptiform discharges at postnatal day (P)14 and the high mortality rate of EEG implantation on infant rats, $P < 10$, we chose P12 rats to start EEG monitoring. It is noteworthy that the generator of epileptiform discharges could not be localized on a small infant rat brain by the scalp/epidural EEG with limited spatial resolution. Therefore, one electrode was implanted on each hemisphere to detect (not localize) epileptiform discharges using the referential montage to the cerebellum. In brief, animals were implanted with four epidural screw electrodes as described previously.[5] To obtain high resolution and quality EEG signals from early postnatal rats, we took advantage of Natus NeuroWorks EEG software and Natus Quantum long-term monitoring (LTM) EEG amplifier, the standard platform for clinical application at the University of Michigan Comprehensive Epilepsy Center. Animals were intermittently monitored for 2-3 hours every 8-12 hours until P18, when animals matured enough to be weaned for continuous monitoring (Figure 1A). Recordings were sampled at 4096 Hz and were analyzed offline with concurrent video-recording. Seizures and epileptiform activity were assessed manually in

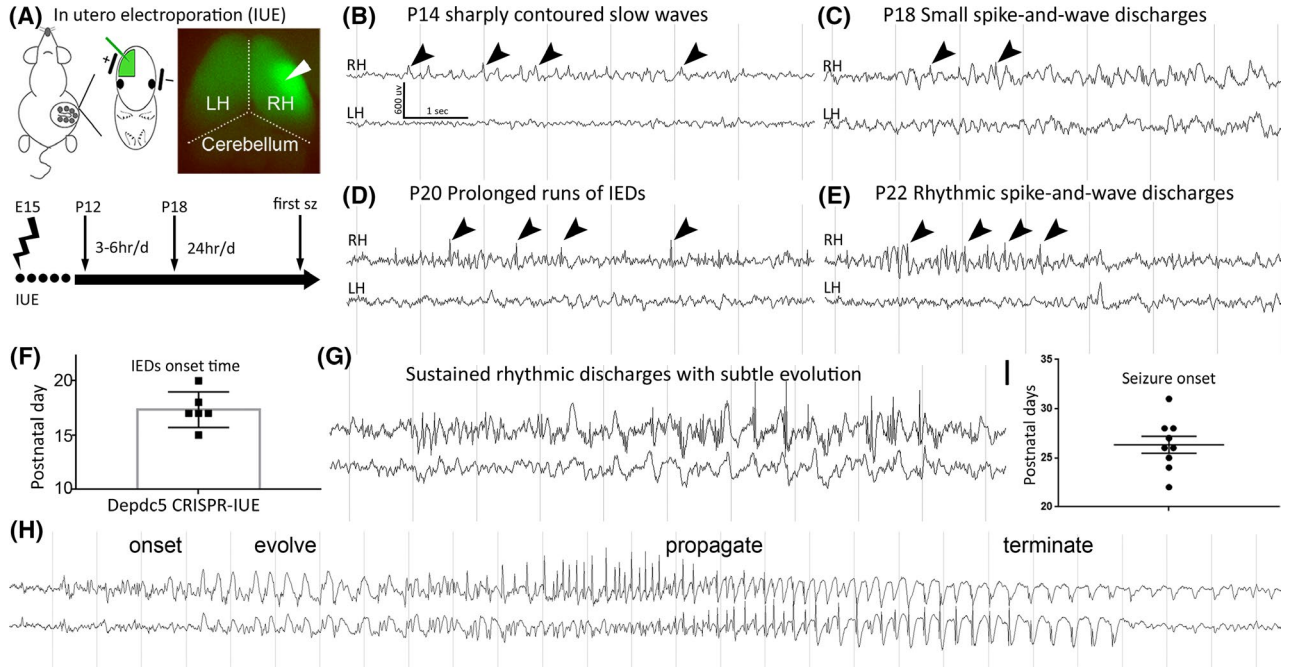

FIGURE 1 Evolution of interictal epileptiform discharges (IEDs) and spontaneous seizures. A. Shown is a diagram of the in utero electroporation (IUE) system. Green fluorescent protein (GFP) plasmids are injected into the lateral ventricles of the rat embryonic brain using a glass microcapillary needle followed by electroporation. On the right, a representative image shows a brain with GFP-IUE. The transfected cortex (arrowhead) displays a bright GFP signal in the right hemisphere (RH). Please see reference[5] for procedure details as well as genetic, pathological, and electrophysiological validation. The procedural timeline: *Depdc5* CRISPR-IUE is performed at embryonic day 15 (E15). Animals are monitored by intermittent EEG recordings [3-6 hours per day starting at postnatal day 12 (P12)] until P18, when 24-hour continuous EEG monitoring can be started. B. Runs of rhythmic or quasi-rhythmic sharply contoured delta activity (arrowheads) start emerging as early as P15 over the hemisphere (RH) with dysplasia, which is not seen over the contralateral hemisphere (LH, left hemisphere) or in control CRISPR-IUE rats (data not shown here). C. At P18, ill-formed EDs are seen in the same animal. D. At P20, better-formed spikes and S-Ws that are short-lived and fragmented with a hint of periodicity. E. By P22, frequent and sustained rhythmic spike-and-wave (S-Ws) are seen in the dysplastic hemisphere. F. Quantification shows that the median age of EDs emergence is P17 (n = 6). The minimal and maximal age of ED appearance is P15 and P20, respectively. G. Following runs of prolonged (>5 s) rhythmic discharges that likely are in the continuum of previous identified EDs, ictal- and interictal spectrum events gradually build up the duration and rhythmicity and finally blossom into (H) clear ictal events with well-defined evolution in morphology, space, and frequencies. I. The median and minimal age at first seizure is P26 and P22, respectively.

their entirety by two fellowship-trained and board-certified epileptologists (Drs. Mihaylova and Wang) blind to experiments and one postdoctoral fellow (Dr. Hu) who was extensively trained for EEG reading. Epileptiform patterns are described as transients distinguishable from background activity with a characteristic morphology typically, but neither exclusively nor invariably, found in the interictal EEG recordings of people with epilepsy.[14,15] Epileptiform patterns have to fulfill at least three of the following five criteria: (1) Sharp wave or spike morphology (<200 msec duration); (2) standing out from the background activity (frequency or amplitude); (3) asymmetry of the waveform: a sharply rising ascending phase and a more slowly descending phase, or vice versa; (4) the transient is followed by an associated after-going slow-wave; (5) the background activity surrounding epileptiform discharges is disrupted by the presence of the epileptiform discharges. Here, we did not use rodent EEG criteria, which often requires the amplitude of epileptiform discharges to be three times higher than the baseline activity.[16,17] Upon record reviewing, we concluded that the traditional rodent epileptiform criteria would misinterpret subtle interictal epileptiform discharges obtained in our platform (data not shown). Seizures are defined as EEG phenomena consisting of repetitive epileptiform EEG discharges at >2 cycles/second and characteristic patterns with quasi-rhythmic spatiotemporal evolution (ie, gradual change in frequency, amplitude, morphology, and location), lasting at least several seconds (usually >10 s). EEG seizure patterns unaccompanied by behavioral epileptic manifestations are referred to as electrographic or subclinical seizures.[14,15]

2.3 | Local field potential recording

Depdc5 CRISPR-IUE rats at 2- to 3-months-old were implanted with recording electrodes (Nichrome wire, 0.003", StablOhm

675, California Fine Wire Company, CA) to record local field potentials (LFPs). The impedances of electrodes were 0.44-0.48 MΩ. Animals were anesthetized with 5% (induction) then 2%-3% (maintenance) isoflurane. After scalp incision and skull exposure, the dysplastic cortex was identified by a house-made fluorescence lamp. Paired electrodes were placed in the neocortex (1 mm tip separation) in four categories of locations: (1) the core/center of identified dysplastic cortex under fluorescence lamp; (2) peripheral sites of and (3) sites outside the dysplastic cortex; and (4) homologous cortex in the contralateral hemisphere. Electrode wires and connectors were embedded in dental acrylic. The animals recovered from surgery for at least 7 days before recording was started. Recordings were made during free wake and sleep behavior in a chamber with free access to water and food. Due to animal welfare and regulation, intermittent instead of 24-hour continuous recordings were performed on six rats, of which each underwent from 782 to 2292 minutes monitoring in 3-5 days (Suppl. Table 1). Electrophysiological signals were acquired at 20 kHz (RHD recording controller, Intan Technologies, CA) and then low-pass filtered and downsampled to 1250 Hz, band-pass filtered 0-450 Hz for LFP analysis, and band-pass filtered 300-9000 Hz for multiple unit activities by using a combination of custom code in MATLAB (Natick, MA), a Buzsaki laboratory code library: 'buzcode' (https://buzsakilab.com/wp/resources/buzcode/) and a Watson laboratory code library, and custom MATLAB codes. Video recordings were made simultaneously with electrophysiological recordings for identifying behavioral effects.

2.4 | LFP analysis

The signals from the first 20 minutes of recovery from isoflurane were not analyzed in order to exclude the effects caused by the anesthesia. Fast Fourier transform analysis used MatLab FFT instruction to analyze the 5-second segment of data with rectangles windowing without overlap. Frequency bands were separated into delta (1-4 Hz), theta (4-8 Hz), alpha (8-13 Hz), beta (13-25 Hz), low gamma (25-50 Hz), high gamma (50-100 Hz), and high-frequency band (100-250 Hz) ranges for the signals recorded from electrodes implanted in the center (C), the periphery (P), adjacent outside (O), and the contralateral homologous region (L) of the *Depdc5* CRISPR-IUE–induced cortical dysplasia.

The background was defined as the state during which no seizure was captured during the hours of recording on a day. A random 1-hour period of recording was selected and divided into 720, 5-second epochs for the Fourier analysis. A 5-second period of recording before seizure onset was defined as the pre-ictal state. To eliminate the artifact signals caused by recording cable or animal's movement, the sum of magnitude (M) at 1-250 Hz in each location (loc), from each 5-second epoch (i), in the states of was calculated as a Z-score according to the equation below, where $M_{Cond,loc,i}$ is the sum of the absolute magnitude in the non-seizure (NonSz), pre-ictal (PreSz), or ictal (Sz) state ($Cond$) for an epoch (i), $\mu_{Cond,loc}$ is the overall mean across epochs of the absolute magnitude in that location during the 1-hour period recorded on another day when no seizure occurred or all pre-seizure and seizure epochs from each animal, and $\sigma_{Cond,loc}$ is the sample standard deviation of background, pre-seizure, or seizure magnitude for that location over those five-second epochs.

$$Z_{Cond,loc,i} = \frac{M_{Cond,loc,i} - \mu_{Cond,loc}}{\sigma_{Cond,loc}}$$

If the Z-score in one of the four locations in an epoch is larger than 3, that LFP signal is considered as an artifact, and that epoch is excluded from the analysis. To examine the effect of Depdc5 malformation on background LFP magnitude in the absence of seizure, for each epoch (i), for each frequency band (F) the sum of the background non-seizure magnitude (M_{NonSz}) recorded in each location (loc), the core, the periphery, and the ipsilateral cortex outside of Depdc5 malformation ($M_{NonSz,F,loc,i}$) was divided by the LFP magnitude in the contralateral cortex at the point corresponding to the location of the core of the malformation ($M_{NonSz,F,contra,i}$).

$$Mratio_{NonSz,F,loc,i} = \frac{M_{NonSz,F,loc,i}}{M_{NonSz,F,contra,i}}$$

The 5-second epochs before and after seizure onset were analyzed to examine the absolute magnitude for frequency bands in the pre-ictal and ictal state compared to the background. The change in magnitude was calculated as a ratio, where $M_{Cond,F,loc,i}$ is the sum of the absolute magnitude in the pre-seizure or seizure condition ($Cond$) for a particular frequency band (F) recorded in each location (loc), for an epoch (i), and $\mu_{NonSz,F,loc}$ is the overall mean across epochs of the log of absolute power in that frequency band and location during the 1-hourr period recorded on another day when no seizure occurred.

$$Mratio_{Cond,F,loc,i} = \frac{M_{Cond,F,loc,i}}{\mu_{NonSz,F,loc}}$$

The means of these ratios were computed for the 60 PreSz, and Sz epochs (12 from each of the five animals), and the means and their standard errors are plotted for each frequency band and location.

2.5 | Immunocytochemistry

Brains were removed and fixed in 4% paraformaldehyde in phosphate-buffered saline (PBS) after transcardial perfusion,

sectioned at 50-80 μm on a vibratome (Leica VT1000S), and processed for immunocytochemistry as free-floating sections. Primary antibodies included mouse anti-pS6 (1:2,000, Cell Signaling #2211) and chicken anti-GFP (1: 1,000, Aves GFP-1020), mouse anti-Npas4 (Neuromad, N408/62). Fluorescently conjugated secondary antibodies (AlexaFluor 488, 594, or 647) were obtained from Molecular Probes, and nuclei were labeled with Bisbenzimide (Molecular Probes H1398).

2.6 | Rodent magnetic resonance (MRI) imaging

MRI was performed at the Animal Imaging Core at the University of Michigan at P60~P90. Experiments were carried out in a 9.4 Tesla horizontal bore scanner (Agilent Technologies, CA, USA), with a two-channel quadrature radiofrequency rat head coil (M2 M Imaging Corporation, OH, USA). Rats were anesthetized with 1.5% isoflurane/air mixture, and body temperature was maintained using a forced-air heating system. T2-weighted anatomical images were collected applying the following parameters: field of view (FOV) = 35 × 35 mm; slice thickness = 0.5 mm; matrix readout direction × phase-encoding direction (RO×PE) = 256 × 128; repetition time (TR) = 4000 msec; and effective echo time (TE_{eff}) = 60 msec. T1-weighted images were collected using the following parameters: FOV =35 × 35 mm; slice thickness =0.5 mm; matrix (RO × PE) = 256 × 128; TR = 710 msec; time to echo (TE) = 17 msec.

2.7 | Patient data, analysis, and MRI-electrode co-registration

Cases were identified from the University of Michigan Comprehensive Epilepsy Centers and included in the analysis if they had a diagnosis of FCDII and underwent a presurgical evaluation using digital intracranial depth- or stereo-EEG recordings between 2014 and 2018. Patients underwent a comprehensive presurgical epilepsy assessment; 1.5- or 3-T MRI three-dimensional T1 and fluid-attenuated inversion recovery (FLAIR) sequences were available for all patients. In a subset of patients, additional examinations were performed with positron emission tomography (PET) using 18F-fluorodeoxyglucose, magnetoencephalography (MEG), and single-photon emission computed tomography (SPECT) using technetium-99. A decision to proceed to SEEG was made at the individual patient level when noninvasive data were discordant and typically when the presumed EZ (or epileptic zone) could not be confidently localized. Cases were discussed at Refractory Epilepsy Conference with epilepsy faculties, neuroradiologists, psychologists, speech pathologists, social workers, and neurosurgeons.

T1-weighted MRI studies (preoperative and postoperative) and a computerized tomography (CT) scan (postoperative) were acquired for each patient to aid in the localization of stereotactically implanted electrodes. The postoperative CT and MRI were registered to the preoperative MRI by the rigid transformation of normalized mutual information using statistic parametric mapping (SPM).[18] Cortical reconstruction and volumetric segmentation of patients' MRI studies were performed using Freesurfer (http://surfer.nmr.mgh.harvard.edu/).[19,20] Electrodes were localized relative to the Freesurfer cortical pial surface using open-source software (available for download online https://github.com/towle-lab/electrode-registration-app/).[21] Each electrode contact was semi-automatically segmented from the CT by intensity value and size and then manually labeled. The coordinates from each electrode contact were then mapped onto pre- and postoperative T1 images to view their locations relative to the pial anatomy in 3D or as individual contacts on MRI slices. Localization of electrodes is confirmed using MRI artifacts elicited on the postoperative MRI.

2.8 | Image acquisition and statistical analyses

Multi-color imaging was performed using a Leica SP5 confocal microscope. All the images were further processed in Adobe Photoshop CS3 software. Statistical analysis was performed using Microsoft Excel and GraphPad. A confidence interval of 95% ($P < 0.01$) was required for values to be considered statistically significant. All data were presented as mean ± standard error of the mean (SE\M) unless noted otherwise. For power spectral analysis, one-way and two-way analyses of variance (ANOVAs) were performed with the Levene homogeneity of variance test and Tukey multiple comparisons test. Graphs were plotted using Prism (Graphpad).

3 | RESULTS

3.1.1 | Evolution of epileptiform discharges and spontaneous seizures in *Depdc5* CRISPR-IUE FCDII rats

As shown in our previous work, we used *Depdc5* CRISPR-IUE to generate FCDII rats, of which 100% developed spontaneous seizures.[5] Pathologically, cytomegaly, increased

phospho-S6 (pS6) immunostaining, and dysmorphic neurons were seen in the dysplastic cortex (data not shown here).[5] However, the latent period or when animals develop their first seizure remains unknown. We first set out to determine when epileptiform discharges (EDs) start emerging. All animals developed clear definitive EDs during the third postnatal week (Figure 1F: median: P17; minimum: P15).

Of interest, sharply contoured rhythmic or quasi-rhythmic delta activity proceeded the definitive EDs over the dysplastic hemisphere (Figure 1B). Although intermittent rhythmic delta activity is nonspecific in many clinical scenarios, the epileptogenicity of temporal or occipital intermittent rhythmic delta activity (TIRDA or OIRDA) has been well documented.[22] In addition, lateralized rhythmic delta activity (LRDA) has also been statistically associated with seizures using continuous EEG monitoring.[23] Next, discrete ill-formed spikes with small amplitude appeared (Figure 1C) and continued to evolve into runs of spike and wave discharges (S-Ws) that were often short-lived and fragmented with a hint of periodicity (Figure 1D). These S-Ws then lasted longer and finally morphed into well-formed rhythmic S-Ws up to several seconds by the end of the third postnatal week (Figure 1E). Because neuronal proliferation, migration, and lamination are completed in the second postnatal week,[24] the emergence and continuous evolution of EDs during the third postnatal week likely represents the underlying developmental changes in epileptogenic substrates, particularly at the synaptic levels.[25]

Next, we hypothesized that FCD animals develop seizures at a much younger age than reported previously.[26-28] With the same platform and protocol described earlier, the first seizure was recorded as early as P22 (median: P26) (Figure 1I). Although no EEG was performed from P0-12 in our studies, it is unlikely that seizures have occurred during this period because (1) no definitive epileptiform discharges were detected between P12 and P15; (2) it took several days for those ill-formed epileptiform discharges to evolve into definitive epileptiform discharges; (3) the first seizure occurred only after the appearance of sustained and rhythmic S-Ws (Figure 1E); and (4) it was only after did prolonged epileptiform discharges with a hint of evolution emerge (Figure 1g) that animals developed clear ictal events with definite evolution in frequency and morphology (Figure 1H). These organized, progressive, and dynamic changes provide a timeframe during which the dysplastic cortex undergoes an epileptogenic transformation in a stepwise fashion to generate ictal events.

3.1.2 | Epileptiform discharges and seizures are localized within the dysplastic cortex

Clinically, localizing the epileptogenic zone is ultimately critical for epilepsy surgery and circuitry targeting. Intracranial EEG (iEEG) is performed to localize the ictal-onset zone to achieve seizure-freedom. MRI is performed to visualize the abnormal structure, which may or may not overlap with the ictal-onset zone detected by iEEG, mainly because the genetic and cellular defects are probably beyond the MRI-visible lesion. This discrepancy has fueled the clinical debate on whether seizures start within the dysplastic cortex or adjacent "perilesional" regions.[29-31] Experimentally, previous work suggested that the hyperexcitable cortex is distant from the malformed cortex in the freeze-lesion model.[32] Because of the relatively limited spatial control in IUE at the embryonic stage, the dysplasia could not be readily identified at the adult stage for in vivo electrophysiology studies. Therefore, we first performed rodent 9.4 T MRIs on *Depdc5* CRISPR-IUE animals but failed to detect dysplasia (Suppl. Figure 1). Although it is well known that 7 T human MRI has superior performance in detecting dysplastic lesions,[33] these negative MR studies were not unexpected because, as compared to the human brain, the small rodent brain volume and voxel size significantly limit the signal-to-noise ratio (SNR).[34]

Our previous study has shown that the *Depdc5* CRISPR-IUE site has clinically relevant pathologies similar to those seen in the dysplastic lesion resected from patients with FCDIIA.[5] Pathognomonic FCDIIA findings in the Depdc5 CRISPR electroporated site include cytomegalic neurons, increased pS6 immunoreactivity, and the accumulation of nonphosphorylated neurofilament SMI32.[5,35] Therefore, based on the extremely high IUE co-transfection efficiency,[36] we designed a customized fluorescent lamp to visualize the dysplastic cortex co-transfected with *Dedpc5* CRISPR and fluorescent protein (FP) plasmids (Suppl. Figure 2A and B). Guided by the bright FP with excellent skull penetrance, chronic recording wires could then be stereotactically implanted to target the center, peripheral, and distant cortex of FCD (Suppl. Figure 2C and D). First, we quantified the distribution of EDs across different recording electrodes in a 60-minute period. EDs presented with different morphology as spike, poly-spikes, or runs of spike-and-wave complex, and they were time-locked with an increase of cortical spiking bursts on MUA analysis (Figure 2B-D). EDs were located primarily within the dysplastic cortex. They also showed a density gradient from the center to the peripheral recording sites (64% vs 20%), suggesting higher epileptogenicity in the center of dysplasia (Figure 2E). During the nonseizure baseline period, there is no difference in LFP magnitude at 1 to 250 Hz among four different locations: the center (C), the peripheral (P), the adjacent outside cortex (O), and the contralateral homologous cortex of the *Depdc5* CRISPR-IUE–induced dysplasia (Figure 2F). To confirm the intrinsic epileptogenicity at the molecular level, we performed immunostaining for neuronal PAS domain protein 4 (Npas4) (Figure 2G-I), a neuron-specific activity-dependent transcriptional factor activated by excitatory synaptic activity.[37]

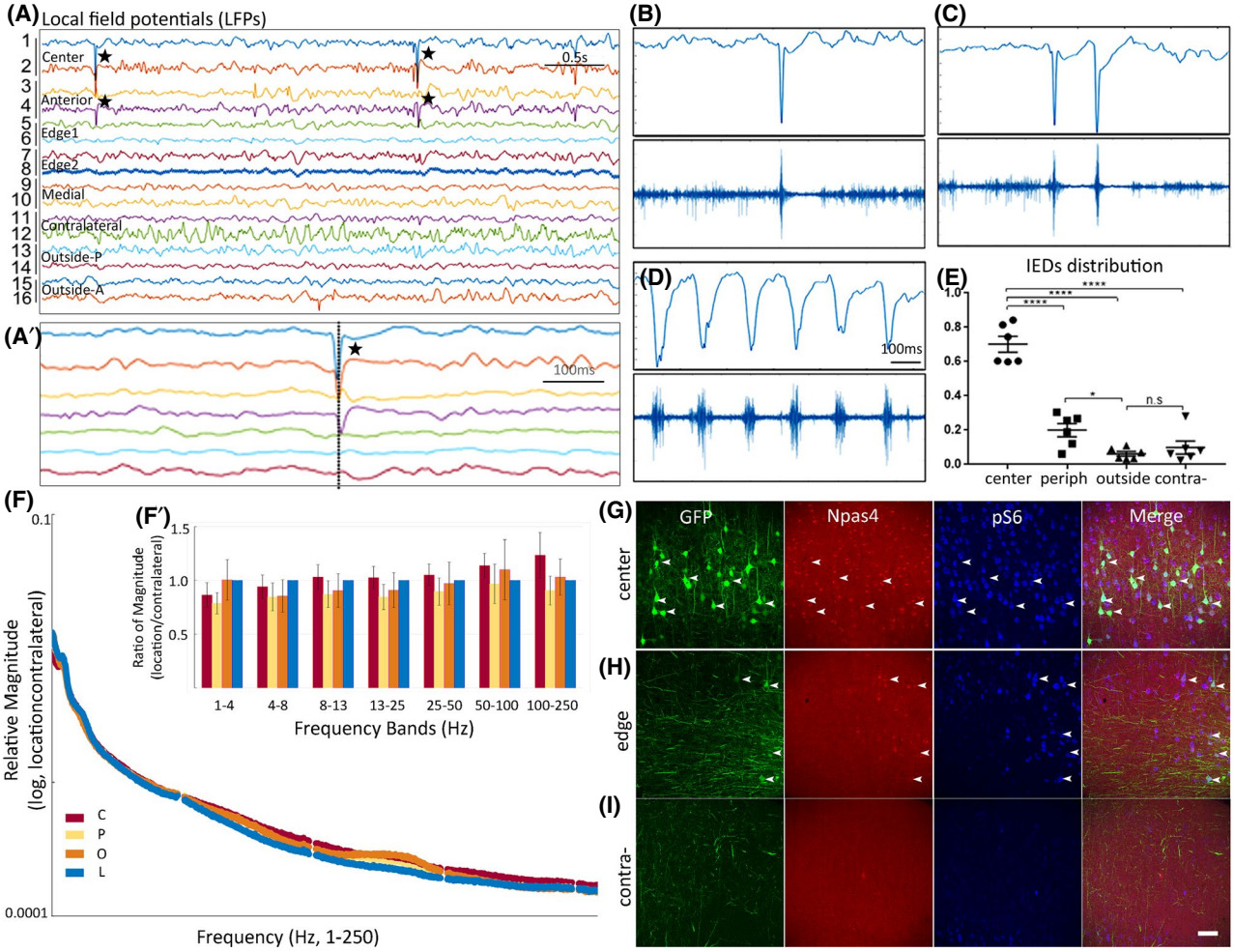

FIGURE 2 Interictal discharges are predominately localized in the dysplastic cortex. A. An example of local field potentials (LFPs) recorded interictal discharges (stars) that are seen only within the dysplastic cortex, with the center having significantly higher amplitude (center: channels 1 and 2; anterior to the center: channels 3 and 4). The implantation strategy is depicted in suppl. Figures 2B-C and 3) Shown is an interictal discharge at an extended time-base. B-D. EDs have different morphology (upper panel) in the same animal (B: single spike; C: polyspikes; D: runs of spike-and-wave discharge), and they are time-locked with a burst of cortical multi-unit activities (MUAs). E. Quantification of EDs at different recording sites (center vs peripheral vs outside vs contralateral) as a percentage of the total number of EDs (arcsine transformation is used to convert percentage numbers for ANOVA test). F. The LFP magnitudes among four locations are similar (one-way ANOVA, $F_{(3, 20)} = 0.367$, $P = 0.778$). C: center; P: peripheral; O: adjacent outside; L: contralateral. F'. There is no significant difference in any particular frequency band: delta (1-4 Hz), theta (4-8 Hz), alpha (8-13 Hz), beta (13-25 Hz), low gamma (25-50 Hz), high-gamma (50-100 Hz), and high frequency (100-250 Hz) (Two-way ANOVA, location: $F_{(3, 140)} = 1.979$, $P = 0.120$; frequency band: $F_{(6, 140)} = 0.731$, $P = 0.626$; interaction: $F_{(18, 140)} = 0.225$, $P = 0.9997$). G. Neuronal PAS domain protein 4 (Npas4), a neuronal activity transcription factor, is significantly increased in the cortex co-transfected with *Depdc5* CRISPR and GFP plasmids. Co-immunostaining of phospho-S6 reveals remarkable mTOR hyperactivation in the transfected cortex. Of note many phospho-S6 (pS6+) neurons are not GFP positive, likely due to the dilution of the non-genome integrating GFP plasmid in rapidly dividing progenitor cells.[5] H. At the edge of the dysplastic cortex, where GFP and *Depdc5* CRISPR co-transfected neurons gradually disappear, both Npas4 and pS6 immunostaining signal starts fading away. I. In the contralateral non-transfected cortex, Npas4 and pS6 immunostaining signals are nearly absent. Arrowheads in G and H indicate transfected neurons and Npas4 staining. Scale bar: 100 μm.

Significantly increased Npas4 staining was observed in the center of the dysplastic cortex (Figure 2G) as compared to the edge of dysplasia (Figure 2H) and nondysplastic cortex (Figure 2I). However, 10% of EDs were independently located in the contralateral homologous cortex, and 5% of EDs in the ipsilateral non-lesional cortex. These "remote" EDs suggest a more extensive irritative or hyperexcitable network induced by "kindling" effects.

Among a total of 157 recorded seizures, 96 seizures (68.44%) started from the center of the dysplastic cortex, and 41 seizures (19.84%) started from the periphery recording sites that were still within the dysplasia (Figure 3A and B).

The remaining 20 seizures (12.74%) started simultaneously from the center and periphery recording sites. Critically, no seizures arose from outside of the dysplasia. During the pre-seizure and seizure periods, LFP absolute magnitude was expectedly greater than the background in both central and peripheral sites but not in the nondysplastic adjacent cortex (Figure 3D-G). These animal data were concordant with our clinical observation in FCD patients who underwent

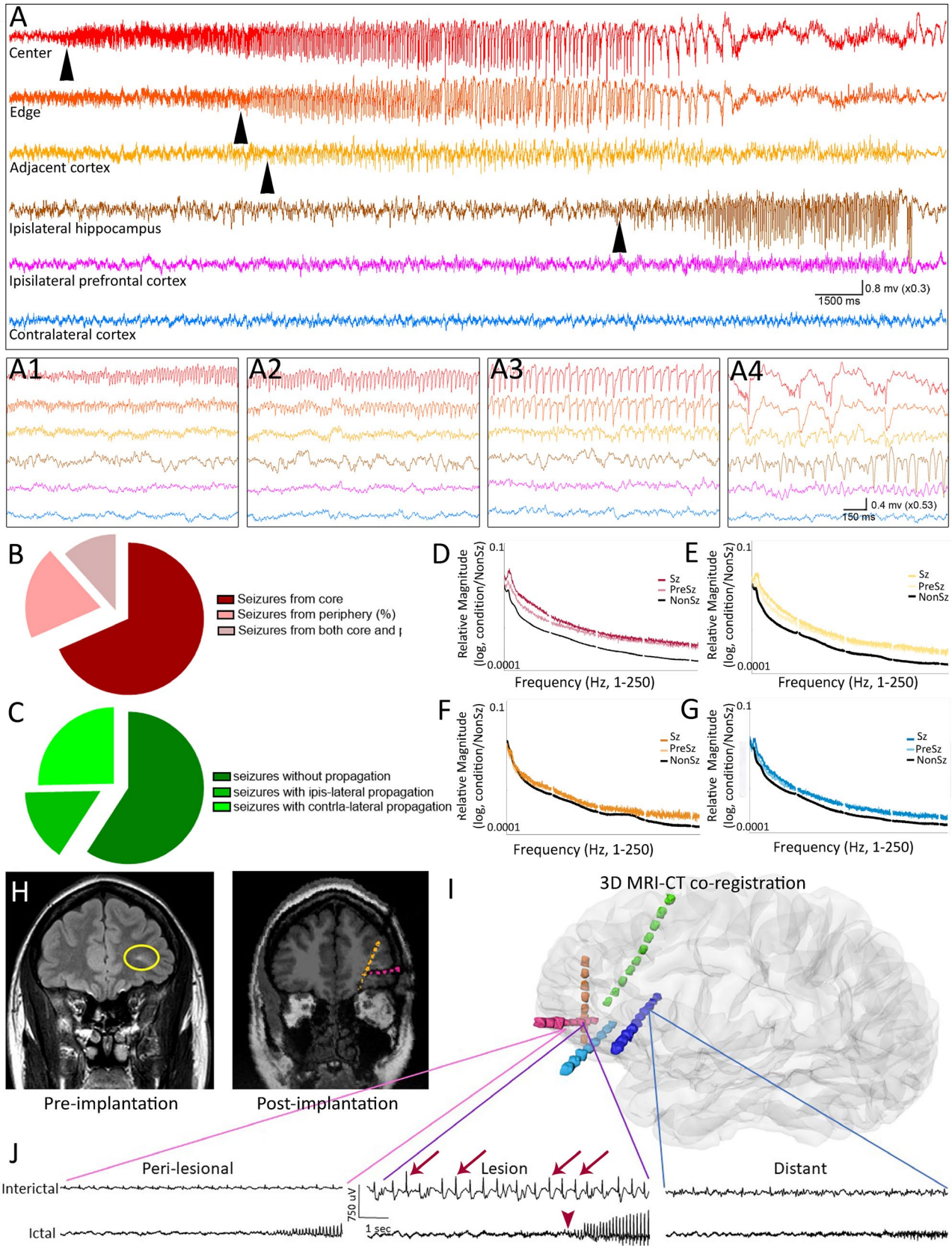

FIGURE 3 Ictal discharges arise within the dysplastic cortex. A. A representative seizure that starts within (A1) the center of the dysplastic cortex and propagates to (A2) the peripheral sites of the dysplastic cortex, (A3) the non-lesional adjacent cortex, and (A4) the ipsilateral hippocampus. B. Approximately 68% and 20% of recorded seizures arise from the center and edge of the dysplastic cortex, respectively. The remaining 12% of recorded seizures arise simultaneously from the center and periphery (Suppl. Table 1). C. Fifty-nine percent of recorded seizures show no propagation, whereas 25% of seizures propagate to the contralateral hemisphere (Suppl. Table 1). D-G. During the period of pre-seizure (PreSz) and seizure (Sz), LFP magnitudes increase significantly as compared to background activity (NonSz) (two-way ANOVA, condition: $F_{(2, 708) =138}.1$, $P < 0.0001$; location: $F_{(3, 708) =61}.42$, $P < 0.0001$; interaction: $F_{(6, 708) =20}.26$, $P < 0.0001$). H-J. Shown is the presurgical evaluation for a young female patient (AA) who developed right frontal lobe epilepsies. H. Pre-implantation magnetic resonance imaging (MRI) shows subtly blurred gray-white matter junction and increased cortical thickness in the left rostral frontal lobe (yellow circle). Post-implantation MRI-computerized tomography (CT) co-registration confirms the location of implanted electrodes that target the dysplasia, adjacent and distant cortices. I. 3D MRI and CT are co-registered to visualize the spatial localization of implanted electrodes. J. Representative intracranial EEG recordings show that both the pacemaker-like IEDs (arrows), a signature of FCD, and ictal-onset (arrowheads) are arising within the dysplasia.

epilepsy presurgical evaluation and intracranial EEG monitoring (Figure 3H-I). A recent study also demonstrated that the cortical tuber has a higher epileptogenic index than the perituberal cortex, nearby cortex, and distant cortex.[38] It is noteworthy that seizure propagation to either ipsilateral or contralateral hemisphere was recorded (Figure 3A, Suppl. Table 1). Although it would be interesting to study anatomo-electroclinical correlation in rat focal epilepsies, the question is beyond the scope of our current study. Besides, our study's implantation strategy aimed to determine the seizure initiation site and, therefore, was not optimized to map the propagation circuits. For example, we did not adequately sample bilateral thalamic and hippocampal structures critical in seizure propagation. It is also challenging, if not impossible, to classify focal seizure semiology in rodents accurately.

4 | DISCUSSION

Recently, focal cellular and molecular pathologies of FCDII have been generated using in utero electroporation (or IUE) to activate mTOR signaling pathways.[26-28,39-41] However, these studies did not investigate either the latent period of epileptogenesis or the ictal-onset site.

4.1.1 | The latent period and epileptogenesis

Because seizure itself provokes sustained and widespread cellular and molecular responses,[2] a defined latent period provides a critical time-window to investigate the mechanism of epileptogenic processes that take place before epilepsy onset. It has been shown that many biochemical, transcriptional, and functional changes in Tsc1-KO neurons arise secondarily due to seizures.[42] Unfortunately, the latent period remains an enigma, if not unknown, in human epilepsies and experimental animal models[43] because (1) Human samples are obtained from patients with severely drug-resistant seizures that have already generated widespread cellular, molecular, and circuitry alterations. (2) The first seizure heralding the onset of epilepsy may not be clinically disruptive unless a tonic-clonic seizure or an overt complex partial seizure is observed. (3) The speculative latent period before the first seizure in animal studies has been repeatedly entrenched by discontinuous seizure monitoring methods. For example, Loscher et al. identified only one study that used continuous (24/7) epidural EEG in a controlled cortical impact (CCI) traumatic brain injury (TBI) mouse model.[43] (4) Nonconvulsive seizures in rodents, as shown by our previous study, often present as motionless staring and are challenging to be detected by simple behavioral observation.[5] Because of these challenges and pitfalls, previous mechanistic studies using experimental FCD models actually were investigating the period during which seizures probably have already been well-established. For example, Lim et al., in their seminal paper, determined that the seizure-onset time in the mTOR mutant IUE mice was ~6 weeks, but they only started video-recording without EEG (12 hours per day) at P21 to monitor behaviorally visible tonic-clonic seizures.[27] Similarly, Hsieh et al. only started performing EEG in 2-month-old animals in the mutant Rheb IUE models.[28] Gene profiling studies from these studies or human resected tissues probably at most demonstrated epiphenomenal phenotypes (either pro- or anti-epileptic) in epileptic brains.[8,9] Our research took advantage of a novel FCDII rat model to establish the latent period and showed that EDs emerged as early as ~P15 and preceded the very first seizures. These EDs occurred initially as ill-formed spikes with a small amplitude and then gradually evolved into S-Ws with a more complex appearance and more sustained rhythmicity. A majority of animals developed their first seizures during the fourth week (P22-28), much earlier than reported previously.[27,28]

In the previous mouse *Depdc5* CRISPR-IUE study, the continuous EEG monitoring from P21-90 showed that 30% (4/14) of mice developed the first seizure by the second month (P37-54, median P44), and three mice died of SUDEP-like events after a single seizure.[40] Species differences might explain the discrepancies in seizure onset, prevalence, and frequency. Although sudden unexpected death in epilepsy (SUDEP) has also been reported in patients with

DEPDC5 mutations,[44,45] we did not observe SUDEP-like events in *Depdc5*-IUE rats (n ≥ 6) during a 12-month period (one death from both FCD and control groups).

4.1.2 | Intrinsic epileptogenicity in focal cortical dysplasia

Clinically, whether seizures start within the dysplastic cortex or adjacent "perilesional" regions or more distant structures that are part of the epileptogenic network remains controversial.[29-31,46-49] Penfield and Palmini proposed the concept of perilesional epileptogenicity based on electrocorticography (ECoG) recordings of spikes in perilesional regions of cortical scars or tumors.[46,47] In addition, direct recordings from within and around tubers in tuberous sclerosis complex (TSC) patients suggest that the perituberal cortex generates seizure activity.[29,48,49] However, the highly epileptogenic discharges over or within the dysplastic cortex in other studies argue for intrinsic epileptogenicity.[30,31] These conflicting data, at least, are in part due to MRI being unable to identify dysplastic cortex at the cellular and genetic levels adequately. For example, pathological studies of the MRI-defined perituberal cortex have revealed mTOR hyperactivation, increased axonal connectivity, and dysplastic cells.[38,50-52] Experimentally, without a defined ictal-onset site, it would be nearly impractical to construct the circuitry and molecular network underpinning the ictogenesis that have distinctly different mechanisms from those in seizure-propagating sites. The seizure-onset site in existing FCD animal models has not been investigated at all.[26-28,40,53] Our data for the first time showed intrinsic epileptogenicity in a highly clinically relevant FCD model that displays an epileptogenicity gradient from the center of the dysplastic cortex to the peripheral, concordant with our clinical data and recent studies on tuberous sclerosis (TS) patients.[38]

However, several important questions remain unanswered. First, whether the epileptogenic network evolves over time could not be answered by current recording techniques, since the duration of intracranial LFP recording is limited to several days to a few weeks. It is plausible that adjacent "normal cortex" could be continuously recruited to the epileptogenic network. Second, high-frequency oscillation (HFO), ictal-onset, and ED patterns at the center and peripheral sites of dysplasia could be further compared and analyzed, which, in combination with human data, would help decision-making in epilepsy surgery for patients with FCDII. Finally, the mechanisms of delayed onset of epilepsy are unknown. Why do animals with brain somatic mutations at the mid-embryonic stage only develop seizures during the fourth postnatal week? Detailed molecular profiling during the identified latent period may lead to mechanistic-based therapies.

In summary, our studies answered two conceptually critical questions, providing a well-defined latent period and ictal-onset site to investigate the epileptogenic pathogenesis at molecular, cellular, and circuitry levels. Our studies also provide a technical platform to study other focal epilepsies, such as FCDI and brain tumor–related epilepsies.

ACKNOWLEDGMENTS

Y.W. received funding from NIH (K08NS099379, R01NS113824, U54NS117170). S.H. received funding from the Wisdom Accumulation and Talent Cultivation Project of the Third Xiangya Hospital of Central South University and China Postdoctoral Science Foundation (2020M672519).

AUTHOR CONTRIBUTIONS

Y.W. contributed to the conception and design of this study. All authors contributed to the acquisition and analysis of data. Y.W drafted the text.

POTENTIAL CONFLICTS OF INTEREST

Nothing to report.

We confirm that we have read the Journal's position on issues involved in ethical publication and affirm that this report is consistent with those guidelines.

ORCID

Hsin-Yi Kao https://orcid.org/0000-0002-7525-983X
Shuntong Hu https://orcid.org/0000-0001-9179-7411
Yu Wang https://orcid.org/0000-0002-2489-1288

REFERENCES

1. Poduri A, Whittemore VH. The Benchmarks: progress and emerging priorities in epilepsy research. Epilepsy Curr. 2020;20:3S–4S.
2. Represa A. Why malformations of cortical development cause epilepsy. Front Neurosci. 2019;13:250.
3. Luhmann HJ. Models of cortical malformation–chemical and physical. J Neurosci Methods. 2016;260:62–72.
4. Becker AJ, Beck H. New developments in understanding focal cortical malformations. Curr Opin Neurol. 2018;31:151–5.
5. Hu S, Knowlton RC, Watson BO, Glanowska KM, Murphy GG, Parent JM, *et al*. Somatic Depdc5 deletion recapitulates electroclinical features of human focal cortical dysplasia type IIA. Ann Neurol. 2018;84:140–6.
6. Blumcke I, Spreafico R, Haaker G, Coras R, Kobow K, Bien CG, *et al*. Histopathological findings in brain tissue obtained during epilepsy surgery. N Engl J Med. 2017;377:1648–56.
7. Iffland PH, 2nd, Crino PB. Focal cortical dysplasia: Gene mutations, cell signaling, and therapeutic implications. Annu Rev Pathol. 2017;12:547–71.
8. Dibbens LM, de Vries B, Donatello S, Heron SE, Hodgson BL, Chintawar S, *et al*. Mutations in DEPDC5 cause familial focal epilepsy with variable foci. Nat Genet. 2013;45:546–51.
9. Baldassari S, Picard F, Verbeek NE, van Kempen M, Brilstra EH, Lesca G, *et al*. The landscape of epilepsy-related GATOR1 variants. Genet Med. 2019;21:398–408.
10. Sim NS, Ko A, Kim WK, Kim SH, Kim JS, Shim KW, *et al*. Precise detection of low-level somatic mutation in resected epilepsy brain tissue. Acta Neuropathol. 2019;138:901–12.

11. Baldassari S, Ribierre T, Marsan E, Adle-Biassette H, Ferrand-Sorbets S, Bulteau C, *et al*. Dissecting the genetic basis of focal cortical dysplasia: a large cohort study. Acta Neuropathol. 2019;138:885–900.
12. Wolfson RL, Chantranupong L, Wyant GA, Gu X, Orozco JM, Shen K, *et al*. KICSTOR recruits GATOR1 to the lysosome and is necessary for nutrients to regulate mTORC1. Nature. 2017;543:438–42.
13. de Curtis M, Avoli M. Initiation, propagation, and termination of partial (focal) seizures. Cold Spring Harb Perspect Med. 2015 Jul 1;5:a022368.
14. Kane N, Acharya J, Beniczky S, Caboclo L, Finnigan S, Kaplan PW, *et al*. Corrigendum to "A revised glossary of terms most commonly used by clinical electroencephalographers and updated proposal for the report format of the EEG findings. Revision 2017" [Clin. Neurophysiol. Practice 2 (2017) 170-185]. Clin Neurophysiol Pract. 2019;4:133.
15. Kane N, Acharya J, Benickzy S, Caboclo L, Finnigan S, Kaplan PW, *et al*. A revised glossary of terms most commonly used by clinical electroencephalographers and updated proposal for the report format of the EEG findings. Revision 2017. Clin Neurophysiol Pract. 2017;2:170–85.
16. Twele F, Schidlitzki A, Tollner K, Loscher W. The intrahippocampal kainate mouse model of mesial temporal lobe epilepsy: Lack of electrographic seizure-like events in sham controls. Epilepsia Open. 2017;2:180–7.
17. Gelinas JN, Khodagholy D, Thesen T, Devinsky O, Buzsaki G. Interictal epileptiform discharges induce hippocampal-cortical coupling in temporal lobe epilepsy. Nat Med. 2016;22:641–8.
18. Ashburner JaF KJ. Rigid body registration. Human brain function. 2nd ed. Academic Press; 2003.
19. Fischl B, Sereno MI, Dale AM. Cortical surface-based analysis. II: Inflation, flattening, and a surface-based coordinate system. NeuroImage. 1999;9:195–207.
20. Dale AM, Fischl B, Sereno MI. Cortical surface-based analysis. I. Segmentation and surface reconstruction. NeuroImage. 1999;9:179–94.
21. Brang D, Dai Z, Zheng W, Towle VL. Registering imaged ECoG electrodes to human cortex: A geometry-based technique. J Neurosci Methods. 2016;273:64–73.
22. Schmitt SE. Generalized and lateralized rhythmic patterns. J Clin Neurophysiol. 2018;35:218–28.
23. Rodriguez Ruiz A, Vlachy J, Lee JW, Gilmore EJ, Ayer T, Haider HA, *et al*. Association of periodic and rhythmic electroencephalographic patterns with seizures in critically Ill patients. JAMA Neurol. 2017;74:181–8.
24. Gleeson JG, Walsh CA. Neuronal migration disorders: from genetic diseases to developmental mechanisms. Trends Neurosci. 2000;23:352–9.
25. Semple BD, Blomgren K, Gimlin K, Ferriero DM, Noble-Haeusslein LJ. Brain development in rodents and humans: Identifying benchmarks of maturation and vulnerability to injury across species. Prog. Neurogibol. 2013;106–107:1–16.
26. Lim JS, Gopalappa R, Kim SH, Ramakrishna S, Lee M, Kim WI, *et al*. Somatic mutations in TSC1 and TSC2 cause focal cortical dysplasia. Am J Hum Genet. 2017;100:454–72.
27. Lim JS, Kim WI, Kang HC, Kim SH, Park AH, Park EK, *et al*. Brain somatic mutations in MTOR cause focal cortical dysplasia type II leading to intractable epilepsy. Nat Med. 2015;21:395–400.
28. Hsieh LS, Wen JH, Claycomb K, Huang Y, Harrsch FA, Naegele JR, *et al*. Convulsive seizures from experimental focal cortical dysplasia occur independently of cell misplacement. Nat Commun. 2016;7:11753.
29. Ma TS, Elliott RE, Ruppe V, Devinsky O, Kuzniecky R, Weiner HL, *et al*. Electrocorticographic evidence of perituberal cortex epileptogenicity in tuberous sclerosis complex. J Neurosurg Pediatr. 2012;10:376–82.
30. Chassoux F, Devaux B, Landre E, Turak B, Nataf F, Varlet P, *et al*. Stereoelectroencephalography in focal cortical dysplasia: a 3D approach to delineating the dysplastic cortex. Brain. 2000;123 (Pt 8):1733–51.
31. Palmini A, Gambardella A, Andermann F, Dubeau F, da Costa JC, Olivier A, *et al*. Intrinsic epileptogenicity of human dysplastic cortex as suggested by corticography and surgical results. Ann Neurol. 1995;37:476–87.
32. Sun QQ, Zhou C, Yang W, Petrus D. Continuous spike-waves during slow-wave sleep in a mouse model of focal cortical dysplasia. Epilepsia. 2016;57:1581–93.
33. Wang I, Oh S, Blumcke I, Coras R, Krishnan B, Kim S, *et al*. Value of 7T MRI and post-processing in patients with nonlesional 3T MRI undergoing epilepsy presurgical evaluation. Epilepsia. 2020;61:2509–20.
34. Hoyer C, Gass N, Weber-Fahr W, Sartorius A. Advantages and challenges of small animal magnetic resonance imaging as a translational tool. Neuropsychobiology. 2014;69:187–201.
35. Blumcke I, Thom M, Aronica E, Armstrong DD, Vinters HV, Palmini A, *et al*. The clinicopathologic spectrum of focal cortical dysplasias: a consensus classification proposed by an ad hoc task force of the ILAE diagnostic methods commission. Epilepsia. 2011;52:158–74.
36. Bai J, Ramos RL, Paramasivam M, Siddiqi F, Ackman JB, LoTurco JJ. The role of DCX and LIS1 in migration through the lateral cortical stream of developing forebrain. Dev Neurosci. 2008;30:144–56.
37. Bloodgood BL, Sharma N, Browne HA, Trepman AZ, Greenberg ME. The activity-dependent transcription factor NPAS4 regulates domain-specific inhibition. Nature. 2013;503:121–5.
38. Neal A, Ostrowsky-Coste K, Jung J, Lagarde S, Maillard L, Kahane P, *et al*. Epileptogenicity in tuberous sclerosis complex: A stereoelectroencephalographic study. Epilepsia. 2020;61:81–95.
39. Feliciano DM, Su T, Lopez J, Platel JC, Bordey A. Single-cell Tsc1 knockout during corticogenesis generates tuber-like lesions and reduces seizure threshold in mice. J Clin Invest. 2011;121:1596–607.
40. Ribierre T, Deleuze C, Bacq A, Baldassari S, Marsan E, Chipaux M, *et al*. Second-hit mosaic mutation in mTORC1 repressor DEPDC5 causes focal cortical dysplasia-associated epilepsy. J Clin Invest. 2018;128:2452–8.
41. Baek ST, Copeland B, Yun EJ, Kwon SK, Guemez-Gamboa A, Schaffer AE, *et al*. An AKT3-FOXG1-reelin network underlies defective migration in human focal malformations of cortical development. Nat Med. 2015;21:1445–54.
42. Bateup HS, Johnson CA, Denefrio CL, Saulnier JL, Kornacker K, Sabatini BL. Excitatory/inhibitory synaptic imbalance leads to hippocampal hyperexcitability in mouse models of tuberous sclerosis. Neuron. 2013;78:510–22.
43. Loscher W, Hirsch LJ, Schmidt D. The enigma of the latent period in the development of symptomatic acquired epilepsy - Traditional view versus new concepts. Epilepsy Behav. 2015;52:78–92.

44. Bagnall RD, Crompton DE, Petrovski S, Lam L, Cutmore C, Garry SI, *et al*. Exome-based analysis of cardiac arrhythmia, respiratory control, and epilepsy genes in sudden unexpected death in epilepsy. Ann Neurol. 2016;79:522–34.
45. Nascimento FA, Borlot F, Cossette P, Minassian BA, Andrade DM. Two definite cases of sudden unexpected death in epilepsy in a family with a DEPDC5 mutation. Neurol Genet. 2015;1:e28.
46. Penfield W. Pitfalls and success in surgical treatment of focal epilepsy. Br Med J. 1958;1:669–72.
47. Palmini A. The concept of the epileptogenic zone: a modern look at Penfield and Jasper's views on the role of interictal spikes. Epileptic Disord. 2006;8 Suppl 2:S10–15.
48. Major P, Rakowski S, Simon MV, Cheng ML, Eskandar E, Baron J, *et al*. Are cortical tubers epileptogenic? Evidence from electrocorticography. Epilepsia. 2009;50:147–54.
49. Boonyapisit K, Najm I, Klem G, Ying Z, Burrier C, LaPresto E, *et al*. Epileptogenicity of focal malformations due to abnormal cortical development: direct electrocorticographic-histopathologic correlations. Epilepsia. 2003;44:69–76.
50. Wong M. Mechanisms of epileptogenesis in tuberous sclerosis complex and related malformations of cortical development with abnormal glioneuronal proliferation. Epilepsia. 2008;49:8–21.
51. Ruppe V, Dilsiz P, Reiss CS, Carlson C, Devinsky O, Zagzag D, *et al*. Developmental brain abnormalities in tuberous sclerosis complex: a comparative tissue analysis of cortical tubers and perituberal cortex. Epilepsia. 2014;55:539–50.
52. Muhlebner A, van Scheppingen J, Hulshof HM, Scholl T, Iyer AM, Anink JJ, *et al*. Novel histopathological patterns in cortical tubers of epilepsy surgery patients with tuberous sclerosis complex. PLoS One. 2016;11:e0157396.
53. Park SM, Lim JS, Ramakrishina S, Kim SH, Kim WK, Lee J, *et al*. Brain somatic mutations in MTOR disrupt neuronal ciliogenesis, leading to focal cortical dyslamination. Neuron. 2018;99(83–97):e87.

SUPPORTING INFORMATION

Additional Supporting Information may be found online in the Supporting Information section.

How to cite this article: Kao H-Y, Hu S, Mihaylova T, et al. Defining the latent period of epileptogenesis and epileptogenic zone in a focal cortical dysplasia type II (FCDII) rat model. *Epilepsia*. 2021;62:1268–1279. https://doi.org/10.1111/epi.16868